Journal of
APPLIED PACKAGING RESEARCH

RESEARCH ARTICLE

A Method for Generating Random Vibration Using Acceleration Kurtosis and Velocity Kurtosis

Daichi Nakai*
Sankyu Inc.

Katsuhiko Saito
Transport Packaging Laboratory,
Kobe University

ABSTRACT

Random vibration tests for packaging are conducted to confirm safety during shipping by truck. However, there is a difference between the traditional random vibration tests and the real vibrations on the truck bed. One reason for this difference is the shock caused by road roughness. Hence, many studies have been conducted to improve random vibration testing. In these studies, the root mean square, power spectral density, kurtosis, and probability density of acceleration are considered. In this study, we show that the kurtosis and probability density of velocity are also important factors for such tests and propose a new method for generating vibrations with arbitrary kurtosis of acceleration and velocity. By bringing the kurtosis and probability density of velocity closer to those of real vibration, it is possible to conduct more accurate vibration tests.

KEY WORDS

Transportation, Vibration Test, Velocity, Kurtosis, Probability Density

***Daichi Nakai**
Corresponding Author
d.nakai@sankyu.co.jp

INTRODUCTION

Random vibration tests for packaging are conducted to confirm its safety during shipping by truck. However, there are differences between traditional random vibration tests and the real vibrations experienced on the truck bed. One reason for these differences is the shock caused by road roughness, including speed bumps, cracks, and pothole [1]. Hence, many studies have been conducted to improve random vibration testing.

Some researchers have proposed methods focusing on the probability density and kurtosis of acceleration. The probability density of acceleration during traditional random vibration tests has a Gaussian distribution. However, the probability density of acceleration during real transportations is non-Gaussian (high kurtosis value). Hence, methods for controlling the probability density of acceleration during vibration testing have been proposed [2, 3].

Other researchers have proposed methods to divide the truck bed vibration. Singh et al. proposed a method to divide the vibration based on the root mean square (RMS) of acceleration [4]. Griffiths et al. proposed decomposing the vibration by wavelet transformation and then reconstructing it [5]. Zhou et al. proposed to divide the vibration based on a tenth-peak method and a moving crest factor [6].

The factors that are frequently considered in these proposed methods are the RMS, power spectral density (PSD), kurtosis, and probability density of acceleration.

In impact testing for packaging, both maximum acceleration and velocity change are important factors [7]. In earthquake engineering, both maximum acceleration and maximum velocity are correlated with building damages [8]. Hence, velocity is assumed to be an important factor in vibration testing for packaging. However, to our knowledge, no method has yet considered the factors related to velocity in such tests. In this study, we propose a new method for generating vibrations with arbitrary kurtosis of acceleration and velocity and show that the kurtosis and probability density of velocity are both important factors for considering shocks during random vibration testing.

THEORY

Method for generating vibrations

The traditional method for generating random vibrations is expressed as equation (1):

$$a(t) = \sum_{k=1}^{L} A_k \cos(2\pi \Delta f t + \phi_k), \quad (1)$$

where L, A_k, Δf, and ϕ_k are, respectively, the number of frequency components, the amplitude, the frequency resolution, and the kth phase angle. A_k is expressed as equation (2):

$$A_k = \sqrt{2\pi \Delta f P(k\Delta f)}, \quad (2)$$

where $P(k\Delta f)$ is a PSD. In traditional random vibration tests, ϕ_k denotes random numbers ranging from 0 to 2π.

Hosoyama et al. proposed a method focusing upon phase angles to approximate the kurtosis and probability density of acceleration [2]. In this method, ϕ_k is expressed as equation (3):

$$\phi_k = \phi_{k-1} + 2\pi \Delta f t_{gr}(k\Delta f), \quad (3)$$

where t_{gr} $(k\Delta f)$ is the group-delay time. In this study, t_{gr} $(k\Delta f)$ is a random number of which the average value is m and the standard deviation is σ. m is related to the phase at which the maximum acceleration occurs, and σ is related to the envelope curve of vibration. As σ increases, this curve becomes sharper, and the kurtosis of acceleration becomes higher.

Hosoyama et al. only focused on the value of σ. In this study, we also focus on the value of Δf. Δf is related to the period T_d at which the maximum

acceleration occurs. The relationship between Δf and T_d is expressed as equation (4):

$$T_d = \frac{1}{\Delta f} \quad (4)$$

Here, σ and T_d were changed in the ranges of 0.05 to 2.5 and 1 to 16 s, respectively.

Method to estimate velocity

Typically, velocity v can be estimated from acceleration a as equation (5):

$$v_{t+\Delta t} = v_t + (a_t + a_{t+\Delta t})\frac{\Delta t}{2}, \quad (5)$$

where Δt is a sampling period. However, we cannot accurately estimate velocity from the acceleration measured with an accelerometer using equation (5) because of low-frequency noise. In our previous study, we showed a way to more accurately estimate velocity using a low-cut filter [9].

The Fourier transform of acceleration, $A(f)$, is expressed by equation (6):

$$A(f) = \int_{-\infty}^{\infty} a(t)e^{-2i\pi ft}dt \quad (6)$$

That of velocity is expressed by equation (7):

$$V(f) = \frac{A(f)}{2i\pi f} \quad (7)$$

To eliminate low-frequency noise, $V(f)$ is corrected by low-cut filter $L(f)$. The corrected Fourier transform of velocity $V'(f)$ is expressed by equation (8):

$$V'(f) = L(f)V(f) \quad (8)$$

In this study, a third-order Butterworth filter was used as $L(f)$. The third-order Butterworth filter is expressed by equation (9):

$$L(f) = \frac{1}{1 - 2i\left(\frac{f_c}{f}\right) - 2\left(\frac{f_c}{f}\right)^2 + i\left(\frac{f_c}{f}\right)^3}, \quad (9)$$

where f_c is the cut-off frequency. In this study, f_c is 0.5 Hz.

Velocity, $v(t)$, can be estimated by an inverse Fourier transform:

$$v(t) = \frac{1}{2\pi}\int_{-\infty}^{\infty} V'(f)e^{2i\pi ft}\,df \quad (10)$$

Evaluation method

To evaluate shock intensity during vibration, single-degree-of-freedom (SDOF) structures were used. We assumed that SDOF structures were placed directly on the truck bed (Figure 1). The force balance of an SDOF structure is expressed as equation (11):

$$m\left(\frac{d^2y}{dt^2} - a\right) + c\frac{dy}{dt} + ky = 0, \quad (11)$$

where m, c, k, and y are, respectively, the mass, viscosity coefficient, spring constant, and relative displacement between the mass and the truck bed. The impulse response function for the displacement per unit impulse force excitation, $h(t)$, is expressed as equation (12):

$$h(t) = \frac{exp(-\xi\varpi_n t)sin(\varpi_d t)}{\varpi_d}, \quad (12)$$

where ξ, ϖ_n, and ϖ_d are, respectively, the damping factor, undamped natural angular frequency, and damped natural angular frequency of the response [10]. ω_n is expressed as equation (13):

$$\varpi_n = \sqrt{\frac{k}{m}} = 2\pi f_n, \quad (13)$$

where f_n is the natural frequency. In this study, f_n changed in the range of 1 to 200 Hz. ξ is expressed as equation (14):

$$\xi = \frac{c}{2m\varpi_n} \quad (14)$$

In this study, ξ was 0.05. ϖ_d is expressed as equation (15):

$$\varpi_d = \sqrt{1 - \varpi_n{}^2} \qquad (15)$$

y is expressed as equation (16):

$$y(t) = \int_0^t a(\tau)h(t-\tau)d\tau, \qquad (16)$$

where τ is the parameter. Equation (16) can be calculated by Fourier transformation as

$$y(t) = \frac{1}{2\pi}\int_{-\infty}^{\infty} A(f)H(f)e^{2i\pi ft}df, \qquad (17)$$

where $H(f)$ is the Fourier transform of $h(t)$. The acceleration applied inside the SDOF structure a_i is proportional to the relative displacement y:

$$a_i(t) = 4\pi^2 f_n^2 y(t) \qquad (18)$$

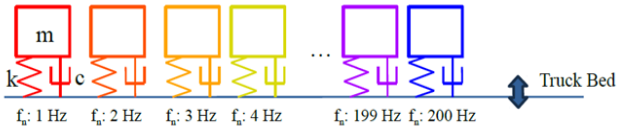

Fig. 1: Schematic diagram of the evaluation.

EXPERIMENT

The vertical vibration data on the truck bed was used as a target. A DER-1000 accelerometer (Shinyei Testing Machinery Co., Ltd.) was fixed to the truck bed. Figure 2 shows the truck and the accelerometer. We ran the truck on the road for 160 s. Figure 3(a), (b), and (c) show, respectively, the acceleration, velocity, and acceleration PSD of real vibration.

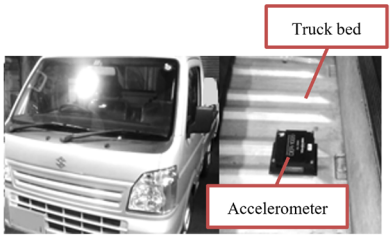

Fig. 2: Truck and accelerometer.

RESULTS AND DISCUSSION

We generated simulated vibrations using the values shown in Figure 3(c) as the target PSD. The vibration generated using random numbers from 0 to 2π is used to simulate random vibration. Vibrations were also generated from equations (1) to (4). Td is set to 1, 2, 4, 8, and 16 s, and σ ranges from 0.05 to 2.5.

All vibrations last 160 s, which is the same time as that for a real vibration. Random vibration lasts 1 s (1000 Hz) per frame and consists of 160 frames. Each frame generated from equations (1) to (4) is taken with a period of T_d. For example, the vibration with a T_d of 1 s consists of 160 frames, and that with a T_d of 16 s consists of 10 frames.

Figure 4 shows the relationship between T_d, σ, and the kurtosis of acceleration. As σ decreased, the kurtosis of acceleration increased. As σ increased, the kurtosis of acceleration decreased and converged to 3, which was the same value as the normal distribution. Even with the same value of σ, the kurtosis of acceleration tends to increase as T_d increases.

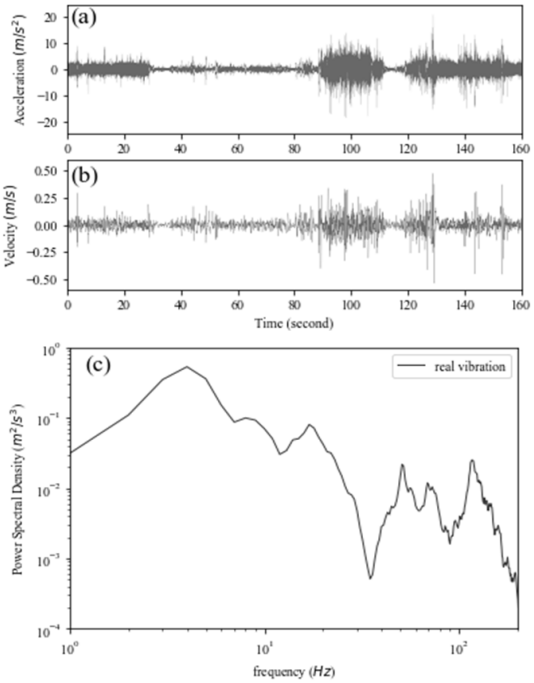

Fig. 3: Real vibration (a) acceleration; (b)velocity; (c)PSD of acceleration.

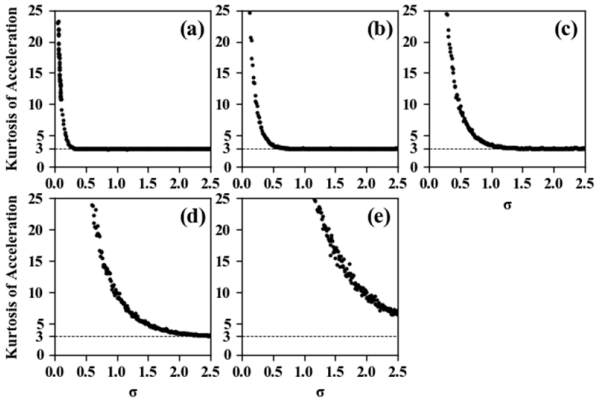

Fig. 4: The relationship between σ, T_d and the kurtosis of acceleration (a) T_d = 1 s; (b) T_d = 2 s; (c) T_d = 4 s; (d) T_d = 8 s; (e) T_d = 16 s.

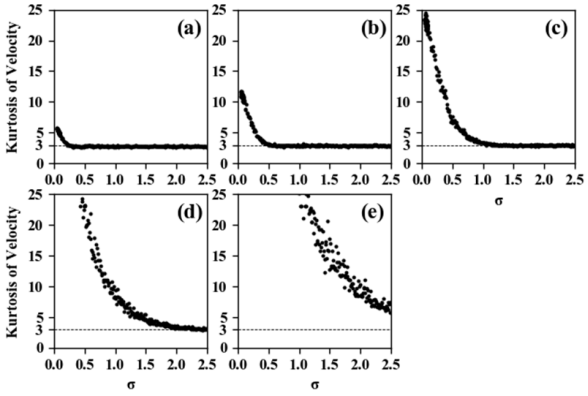

Fig. 5: The relationship between σ, T_d and the kurtosis of velocity (a) T_d = 1 s; (b) T_d = 2 s; (c) T_d = 4 s; (d) T_d = 8 s; (e) T_d = 16 s.

Figure 5 shows the relationship between T_d, σ, and the kurtosis of velocity. As σ decreased, the kurtosis of velocity increased. As σ increased, the kurtosis of velocity decreased and converged to 3, which is the same value as in the normal distribution. The kurtosis of acceleration and velocity showed the same trend.

Figure 6 shows the relationship between the kurtosis of acceleration and that of velocity. When the value of T_d was small, the amount of increase in the kurtosis of velocity was small with respect to that of acceleration. As the value of T_d increased, the amount of increase in the kurtosis of velocity was bigger. Even if T_d increased, the kurtosis of velocity did not significantly exceed that of acceleration.

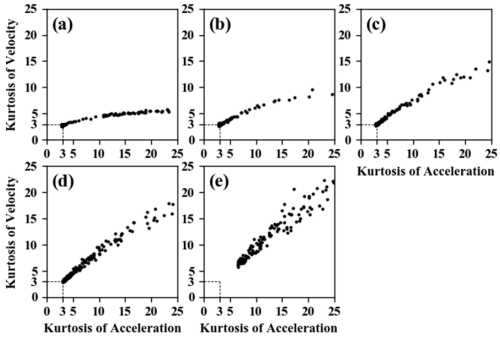

Fig. 6: The relationship between the kurtosis of acceleration and the kurtosis of velocity (a) T_d = 1 s; (b) T_d = 2 s; (c) T_d = 4 s; (d) T_d = 8 s; (e) T_d = 16 s.

To compare in more detail, we extracted the vibrations whose kurtosis of acceleration is close to real vibration. Table shows the statistics of the vibrations. The acceleration kurtosis of extracted non-random vibrations was close to 11.6 (±0.1). On the other hand, the kurtosis of velocity differed for all generated vibrations. The vibration with a T_d of 16 s had a velocity kurtosis close to that of real vibration. Vibrations with T_d values of 1 and 4 s had small velocity kurtosis compared to real vibration.

Table: Vibration statistics.

	Acceleration		Velocity	
	RMS (m/s²)	Kurtosis	RMS (m/s)	Kurtosis
real vibration	1.88	11.61	0.0613	11.90
random vibration	1.90	2.93	0.0701	2.80
T_d = 1 s	1.90	11.67	0.0653	4.66
T_d = 4 s	1.88	11.52	0.0608	9.08
T_d = 16 s	1.90	11.63	0.0624	11.91

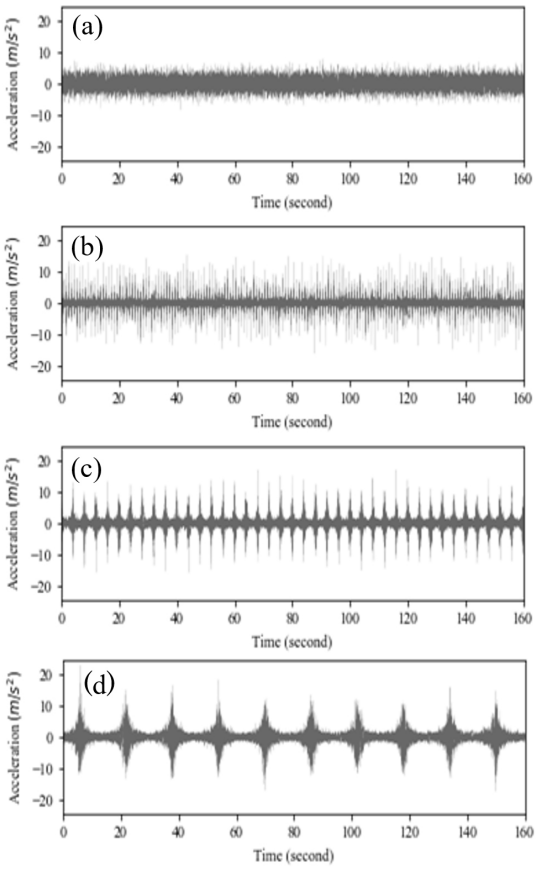

Fig. 7: Time series of acceleration (a) random vibration; (b) T_d = 1 s; (c) T_d = 4 s; (d) T_d = 16 s.

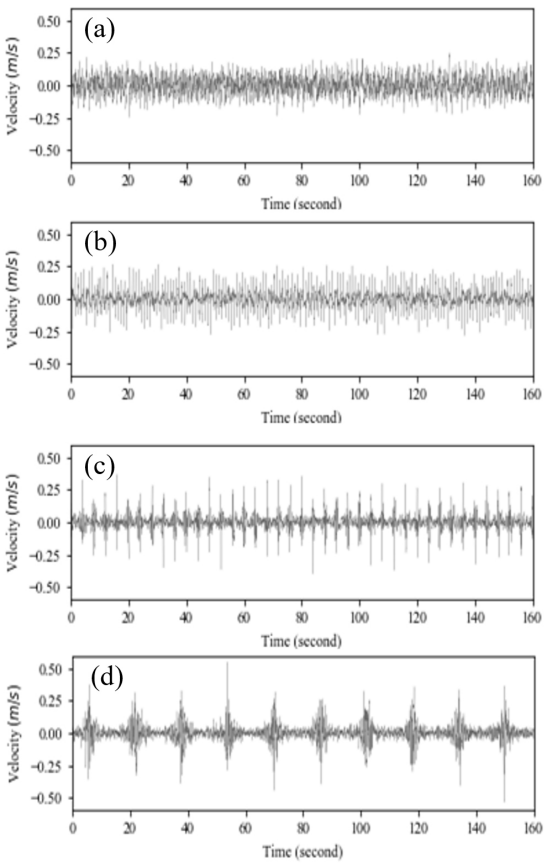

Fig. 8: Time series of velocity (a) random vibration; (b) T_d = 1 s; (c) T_d = 4 s; (d) T_d = 16 s.

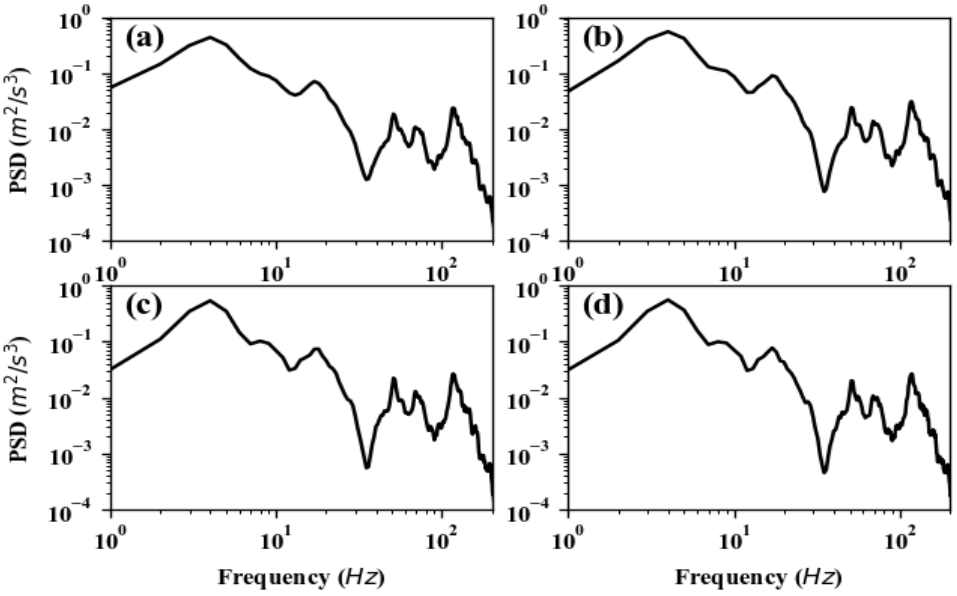

Fig. 9: PSD of acceleration (a) random vibration; (b) T_d = 1 s; (c) T_d = 4 s; (d) T_d = 16 s.

Figure 9 shows the PSD of acceleration. All vibrations had almost the same PSD.

Figure 10 shows the probability density of acceleration. As shown in Figure 10(a), the random vibration, for which kurtosis is close to that of a normal distribution, had a small probability-density-acceleration spread. Other vibrations had nearly the same probability density of acceleration.

Figure 11 shows the velocity probability density. Despite having nearly the same probability density of acceleration, the probability density of the velocity was different from each other. As shown in Figure 11(a), there was a small acceleration probability density spread under random vibration. Figure 11(b) shows that the vibration with a T_d of 1 s closely approximated the spread with random vibration. This was consistent with the kurtosis of the velocity being 4.66, which is close to the normal distribution. The probability densities of the vibration velocity with a T_d of 16 s (Figure 11(d)) and the real vibration (Figure 11(e)) had similar spreads.

Figure 12 shows a_i obtained by equations (12)–(18) when f_n is 5 Hz. As shown in Figs. 12(c) and (d), the period of T_d could be confirmed. However, a period of 1 s could not be clearly confirmed in Fig. 12(b).

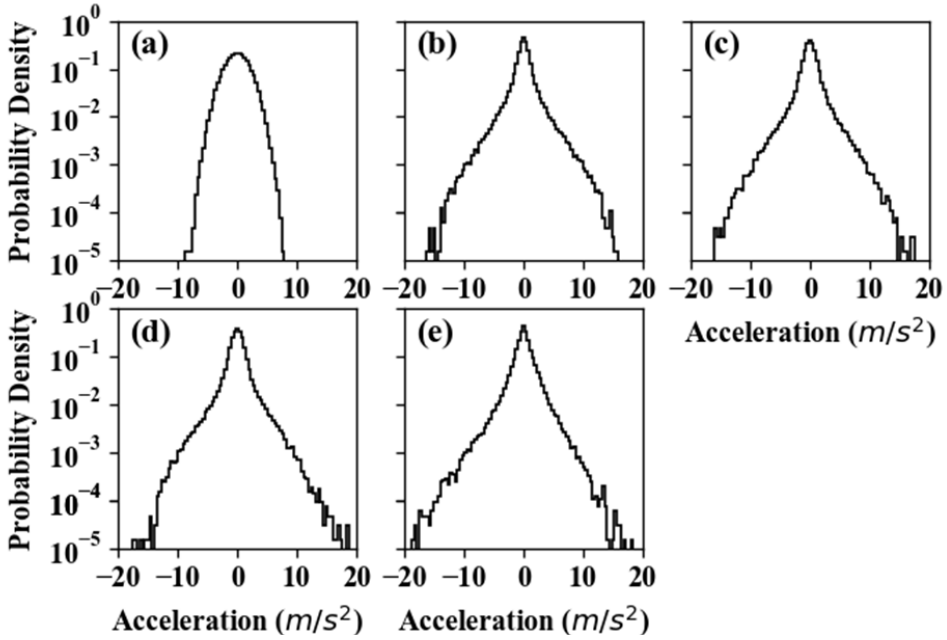

Fig. 10: Probability density of acceleration (a) random vibration; (b) T_d = 1 s; (c) T_d = 4 s; (d) T_d = 16 s; (e) real vibration.

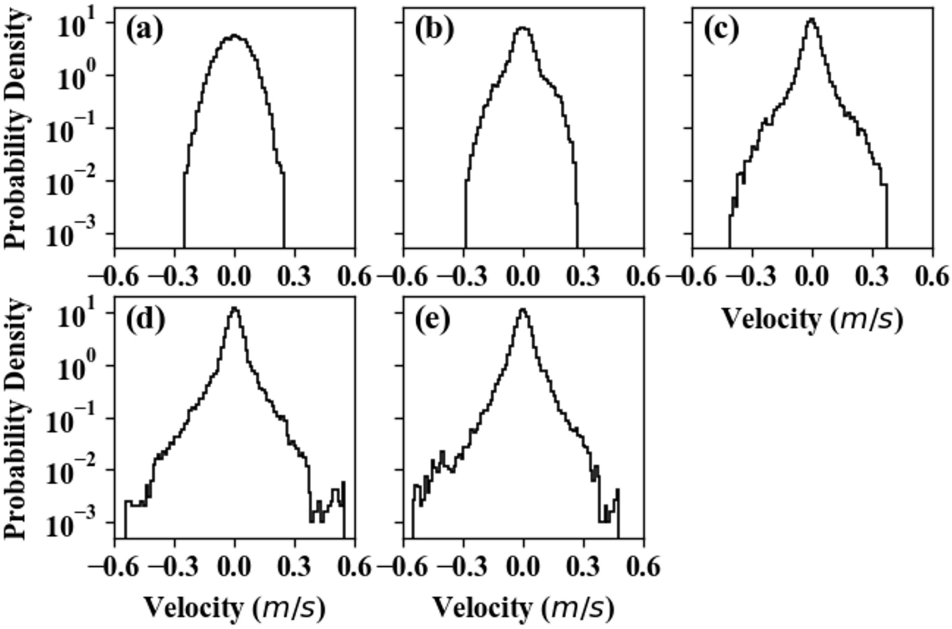

Fig. 11: Probability density of velocity (a) random vibration; (b) T_d = 1 s; (c) T_d = 4 s; (d) T_d = 16 s; (e) real vibration.

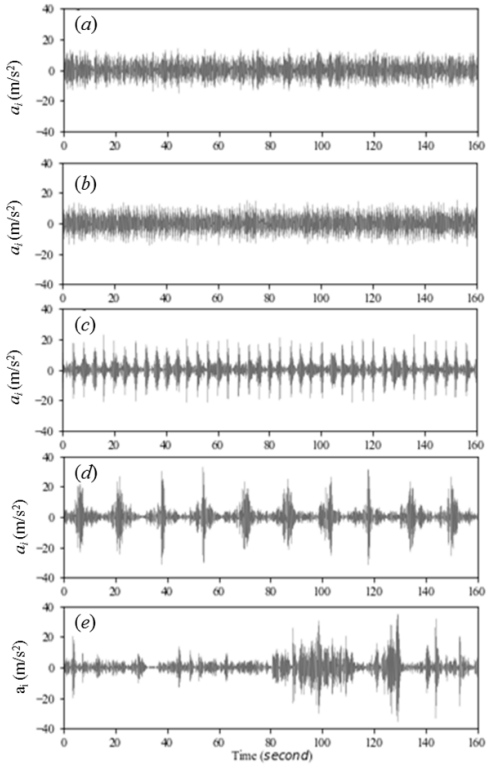

Fig. 12: Time series of a_i when f_n is 5 Hz (a) random vibration; (b) T_d = 1 s; (c) T_d = 4 s; (d) T_d =16 s; (e) real vibration.

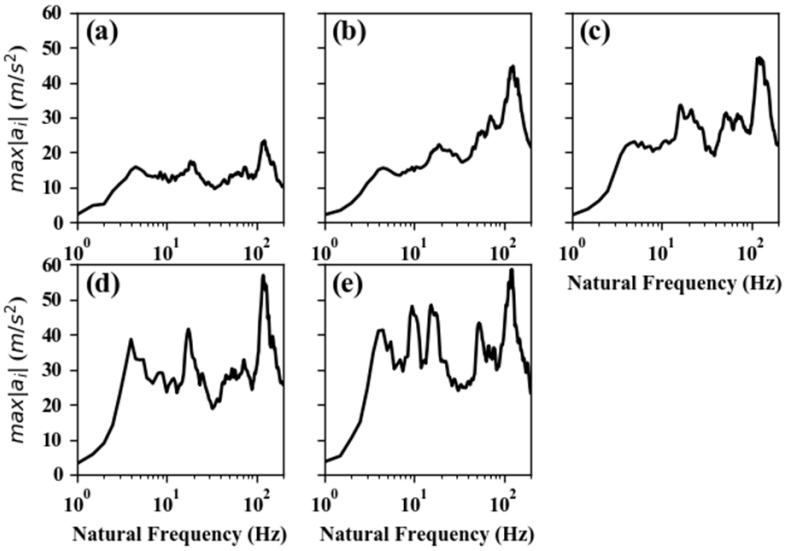

Fig. 13 :The relationship between f_n and max |a_i| (a) random vibration; (b) T_d = 1 s; (c) T_d = 4 s; (d) T_d = 16 s; (e) real vibration.

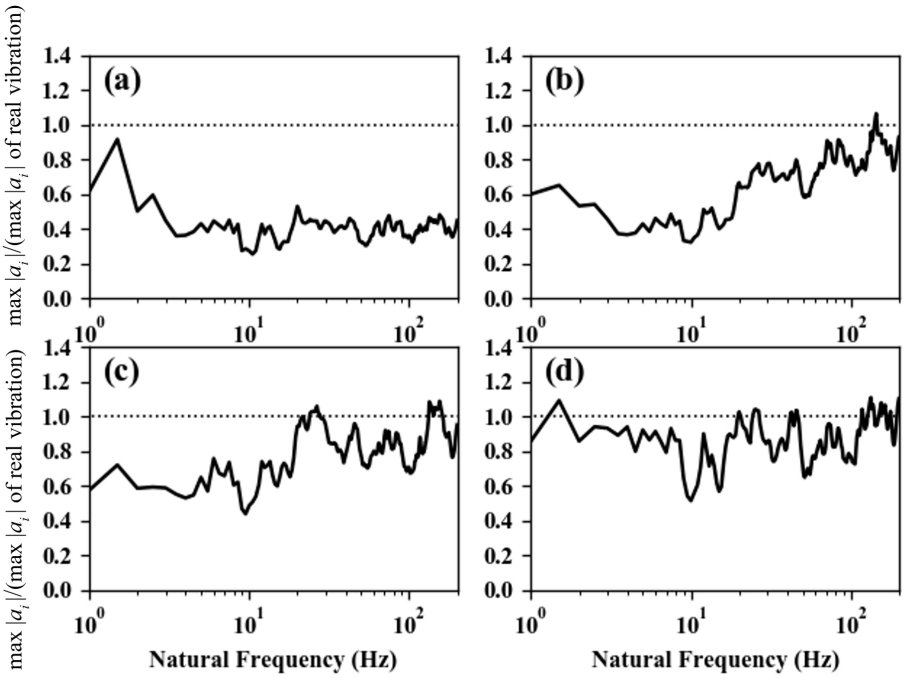

Fig. 14 :The relationship between f_n and max $|a_i|$(real vibration = 1) (a) random vibration; (b) T_d = 1 s; (c) T_d = 4 s; (d) T_d = 16 s.

Figure 13 shows the relationship between the maximum absolute values of a_i (max $|a_i|$) and f_n. It is supposed that, the larger max $|a_i|$ is, the more damage is incurred to packages.

Figure 14 shows max $|a_i|$ divided by max $|a_i|$ of real vibration. Random vibration had a low max $|a_i|$ compared to real vibration in all f_n ranges. Hence, it is supposed that only weak shock occurred during random vibration, as compared to real vibration. As shown in Figs. 14(b)–(d), as T_d increased, max $|a_i|$ divided by max $|a_i|$ of real vibration approached a value of 1.0 in many f_n ranges. The vibration with a Td of 16 s, for which kurtosis was the closest to that of real vibration, also had max $|a_i|$ closest to that of real vibration.

CONCLUSIONS

We generated vibrations with arbitrary kurtosis of acceleration and velocity by changing the factors σ and T_d.

Using this method, we generated vibrations with the same acceleration kurtosis, probability density of acceleration, and PSD, but different kurtosis and probability density of velocity. This showed that the kurtosis and probability density of velocity are important factors for considering shocks during random vibration testing. By bringing the kurtosis and probability density distribution of velocity closer to that of real vibration, it is possible to conduct vibration tests more like real vibrations.

The next task is to verify the effect through actual vibration tests.

REFERENCES

[1] J. Lupine, V. Rouillard and M.A. Sek, "Review paper on road vehicle vibration simulation for packaging testing purposes," Packaging Technology and Science, vol. 28, (8) pp. 657-671, 2015.

[2] A. Hosoyama, K. Saito and T. Nakajima, "Non-Gaussian random vibrations using kurtosis," in Eighteenth IAPRI World Packaging Conference, DEStech Publications, Inc.: San Louis Obispo (CA), USA, 2012.

[3] V. Rouillard and M.A. Sek, "Monitoring and simulating non-stationary vibrations for package optimization," Packaging Technology and Science, vol. 13, (4) pp. 149-156, 2000.

[4] J. Singh, S.P. Singh and E. Joneson, "Measurement and analysis of US truck vibration for leaf spring and air ride suspensions, and development of tests to simulate these conditions," Packaging Technology and Science, vol. 19, (6) pp. 309-323, 2006.

[5] K.R. Griffiths, B.J. Hicks, P.S. Keogh and D. Shires, "Wavelet analysis to decompose a vibration simulation signal to improve pre-distribution testing of packaging," Mechanical Systems and Signal Processing, vol. 76-77, pp. 780-795, 2016.

[6] H. Zhou and Z.W. Wang, "A new approach for road-vehicle vibration," Packaging Technology and Science, vol. 31, (5) pp. 246-260, 2018.

[7] R.E. Newton, "Fragility assessment theory and test procedure," Monterey Research Laboratory Inc., Monterey, California, 1968.

[8] A. Masuda, K. Nagato and H. Kawase, "Study on construction of vulnerability by earthquake response analysis for reinforced concrete buildings," Journal of Structural and Construction Engineering, AIJ, vol. 558, pp. 101-107, 2002. (in Japanese).

[9] D. Nakai and K. Saito, "Estimation method of velocity change on truck bed," Journal of Packaging Science and Technology, Japan, vol. 28, (1) pp. 33-44, 2019. (in Japanese).

[10] Harris' Shock and Vibration Handbook 6th.Edition, 2009; 8.2-8.14.